ACCOUNTS of chemical research

pubs.acs.org/accounts Article

Modeling Interfacial Dynamics on Single Atom Electrocatalysts: Explicit Solvation and Potential Dependence

Zisheng Zhang, Jun Li, and Yang-Gang Wang*

Cite This: *Acc. Chem. Res.* 2024, 57, 198−207 Read Online

ACCESS | Metrics & More | Article Recommendations

CONSPECTUS: Single atom electrocatalysts, with noble metal-free composition, maximal atom efficiency, and exceptional reactivity toward various energy and environmental applications, have become a research hot spot in the recent decade. Their simplicity and the isolated nature of the atomic structure of their active site have also made them an ideal model catalyst system for studying reaction mechanisms and activity trends. However, the state of the single atom active sites during electrochemical reactions may not be as simple as is usually assumed. To the contrary, the single atom electrocatalysts have been reported to be under greater influence from interfacial dynamics, with solvent and electrolyte ions perpetually interacting with the electrified active center under an applied electrode potential. These complexities render the activity trends and reaction mechanisms derived from simplistic models dubious.

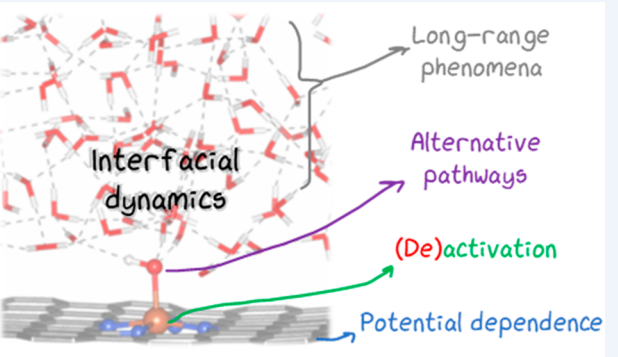

In this Account, with a few popular single atom electrocatalysis systems, we show how the change in electrochemical potential induces nontrivial variation in the free energy profile of elemental electrochemical reaction steps, demonstrate how the active centers with different electronic structure features can induce different solvation structures at the interface even for the same reaction intermediate of the simplest electrochemical reaction, and discuss the implication of the complexities on the kinetics and thermodynamics of the reaction system to better address the activity and selectivity trends. We also venture into more intriguing interfacial phenomena, such as alternative reaction pathways and intermediates that are favored and stabilized by solvation and polarization effects, long-range interfacial dynamics across the region far beyond the contact layer, and the dynamic activation or deactivation of single atom sites under operation conditions. We show the necessity of including realistic aspects (explicit solvent, electrolyte, and electrode potential) into the model to correctly capture the physics and chemistry at the electrochemical interface and to understand the reaction mechanisms and reactivity trends. We also demonstrate how the popular simplistic design principles fail and how they can be revised by including the kinetics and interfacial factors in the model. All of these rich dynamics and chemistry would remain hidden or overlooked otherwise. We believe that the complexity at an electrochemical interface is not a curse but a blessing in that it enables deeper understanding and finer control of the potential-dependent free energy landscape of electrochemical reactions, which opens up new dimensions for further design and optimization of single atom electrocatalysts and beyond. Limitations of current methods and challenges faced by the theoretical and experimental communities are discussed, along with the possible solutions awaiting development in the future.

KEY REFERENCES

- Cao, H.; Wang, Q.; Zhang, Z.; Yan, H. M.; Zhao, H.; Yang, H. B.; Liu, B.; Li, J.; Wang, Y. G. Engineering Single-Atom Electrocatalysts for Enhancing Kinetics of Acidic Volmer Reaction. *J. Am. Chem. Soc.* **2023**, *145*, 13038−13047.[1] This work suggests that charge at the metal center dictates the orientation of interfacial water at the transition state, leading to different acidic Volmer kinetics.
- Chen, J.-W.; Zhang, Z.; Yan, H.-M.; Xia, G.-J.; Cao, H.; Wang, Y.-G. Pseudo-Adsorption and Long-Range Redox Coupling during Oxygen Reduction Reaction on Single Atom Electrocatalyst. *Nat. Commun.* **2022**, *13*, 1734.[2] ORR on an Fe single atom electrocatalyst can undergo a dissociative pathway and generate pseudo-adsorbed hydroxide species, which stay a few water layers away from the interface due to solvation stabilization.

Received: September 17, 2023
Revised: December 9, 2023
Accepted: December 11, 2023
Published: January 3, 2024

- Cao, H.; Zhang, Z.; Chen, J.-W.; Wang, Y.-G. Potential-Dependent Free Energy Relationship in Interpreting the Electrochemical Performance of CO_2 Reduction on Single Atom Catalysts. *ACS Catal.* **2022**, *12*, 6606−6617.[3] Potential-dependent free energy calculations reveal the stepwise nature of CO_2 activation on a single-atom site and better predict potential-dependent activity and selectivity.
- Qian, S.-J.; Cao, H.; Chen, J.-W.; Chen, J.-C.; Wang, Y.-G.; Li, J. Critical Role of Explicit Inclusion of Solvent and Electrode Potential in the Electrochemical Description of Nitrogen Reduction. *ACS Catal.* **2022**, *12*, 11530−11540.[4] Solvation effect and potential dependence are critical for stabilizing the key reaction intermediate and determine the reaction pathway of nitrogen reduction.

1. INTRODUCTION

Since the first report of an "atomically dispersed catalyst" in 1999[5] and the coinage of the term "single atom catalyst" (SAC) in 2011,[6] this family of catalysts has become a hot research topic in various fields, from energy and environmental applications to fundamental surface sciences. An especially successful branch of SACs is the single atom electrocatalysts (SAEs), which consists of single-atom active sites uniformly dispersed on a conducting support, so that they can be used to catalyze electrochemical reactions. Such structural constructs can maximize the atom efficiency, making full use of the supported element.[7] Moreover, the strong interaction between the supported single-atom sites and the underlying substrate is usually accompanied by significant charge transfer, leading to distinct reactivities from their bulk counterparts. These behaviors allow rational construction of active sites based on earth-abundant transition metals with performance comparable to noble metal-based catalysts.

Benefiting from the aforementioned merits, SAEs have quickly become game changers in the field of electrocatalysis, boasting extremely high activity and selectivity toward various electrocatalytic reactions.[8−11] The merit of SAEs lies in not only their reactivity but also their uniformly dispersed active sites, whose exact structures and local environments can be resolved by various characterization methods. With this respect, SAEs also serve as perfect model systems for fundamental studies where experiment and theory can join hands to investigate the mechanisms of various key catalytic reactions.

Compared to the advances in characterization techniques and instrumentation, the development of computational models for SAEs has been more stagnant in the past decade: the computational hydrogen electrode (CHE) is still the most popular go-to choice of the SAE research community, thanks to its simplicity and relatively low computational cost. Although the CHE model has been used to predict the activity trend of some SAE systems with decent accuracy, it has also failed on many others.[12] The inconsistent and system-dependent performance of the CHE for SAEs can be attributed to its underlying assumptions such as linear scaling relationships and thermodynamics-determined overpotentials. Such oversimplifications have been proven to be dangerous and misleading if used indiscriminately, especially for systems limited by kinetics.[13]

Therefore, it is crucial to scrutinize the reaction energetics with a proper consideration of realistic factors. Electrochemical reactions takes place at an electrified electrode/electrolyte interface, with the reaction intermediates under the influence of the dynamic solvent environment, electrolyte ions, the varying electrode potential, and so on.[14] Moreover, many of the realistic factors can be interdependent on each other, with different extents of coupling, giving rise to intricate interplay, which further complicates the modeling.

In this Account, we will review the current state of realistic modeling of SAEs, based on a collection of recent works, including our own contributions, with a focus on the aqueous systems where the interfacial dynamics and local solvation environments play a critical role in determining the kinetics, thermodynamics, potential dependence, and even the reaction pathway of the electrocatalytic reaction. We also critically examine the challenges and limitations associated with the current "state-of-the-art" methods and propose some promising future directions to address these issues.

2. POTENTIAL DEPENDENCE OF THE REACTION FREE ENERGY PROFILE

Quantifying the potential dependence of the reaction free energies and barriers is necessary for understanding the reactivity of SAEs or any electrocatalytic systems. However, the CHE model usually assumes that the potential dependence of reaction free energies follows a simple linear potential dependence of 1 eV per volt. In the cell- and charge-extrapolation schemes of the extended CHE model,[15,16] the free energy barriers at different electrode potentials are calculated based on the same transition state (TS) geometry, with usually insufficient explicit solvation. However, for reactions involving intermediates that are highly polar or can form hydrogen bonds with water, the free energy profile can reshape dramatically. Due to the dynamic nature of the hydrogen bond network within water, it is crucial to perform sufficient configurational sampling to obtain accurate energetics. For example, by ab initio molecular dynamics (AIMD) simulation combined with constrained MD sampling and full explicit solvation treatment, we found that the reaction free energy landscape of $*N_2 \rightarrow *NNH$ on graphitic carbon with embedded FeN_4 SA sites (FeN_4/C), the first step of the nitrogen reduction reaction (NRR), reshapes significantly at different electrode potentials (Figure 1).[4] The reaction free energy and barrier do not linearly correlate with the electrode potential, with a huge boost in both thermodynamics and kinetics as the

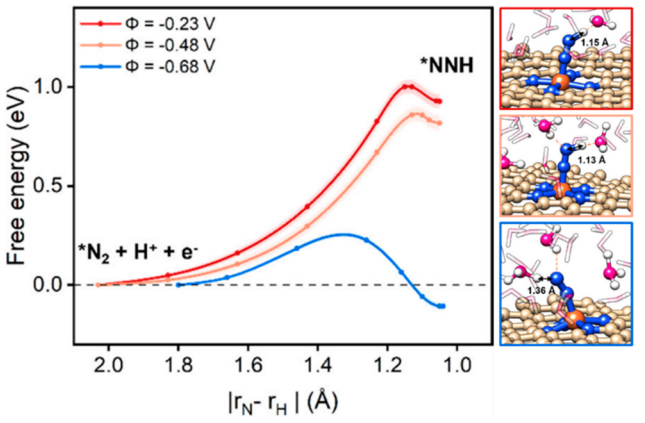

Figure 1. Free energy profiles of N_2 activation on FeN_4/C electrocatalyst at −0.23 V, −0.48 V, and −0.68 V. The corresponding final state geometries are shown on the right. Reproduced with permission from ref 4. Copyright 2022 American Chemical Society.

https://doi.org/10.1021/acs.accounts.3c00589
Acc. Chem. Res. 2024, 57, 198−207

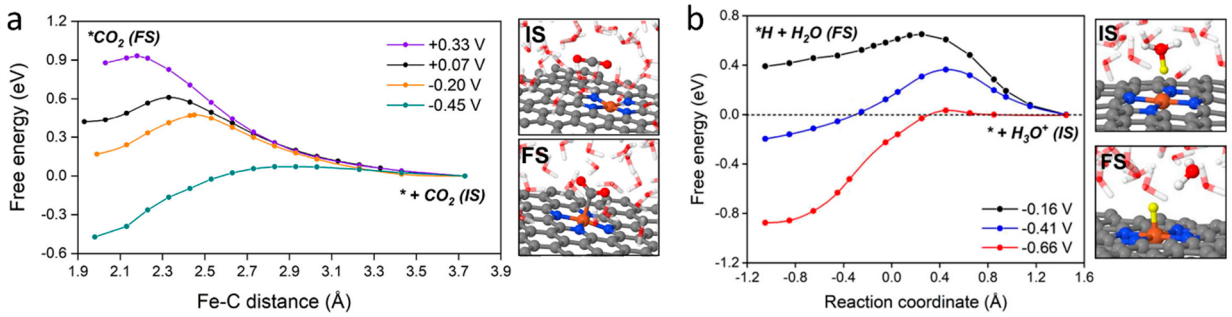

Figure 2. Free energy profiles of (a) CO_2 electro-activation and (b) *H desorption on FeN_4/C. Reproduced with permission from ref 3. Copyright 2022 American Chemical Society.

electrode potential goes from −0.48 V to −0.68 V. More intriguingly, the relative location of the TS along the reaction profile is also dependent on the electrode potential, with the TS at −0.68 V being much closer to the initial state (IS) compared to the cases at more positive potentials. Using the free energetics obtained from AIMD free energy sampling, the overpotential of NRR is predicted to be around 0.7 V, which is much more consistent with experimental observations than the prediction of CHE model (less than −1 V). Those dramatic changes of the reaction free energy profile are due to the response of the interfacial solvation structure to varying potentials: as the waters in the contact layer rearrange, their highly directional hydrogen bond interactions with the reaction intermediate would evolve in a rather unpredictable way, causing nonlinearity in the potential dependence of the free energetics and changing the TS location in the reaction profile.

Including the solvation environment explicitly is also the key to understanding the selectivity trends of electrocatalytic reactions on SAEs. The CO_2 reduction reaction (CO_2RR) is subject to competition with the hydrogen evolution reaction (HER) in negative potential regimes, and the potential dependent selectivity has not been well understood by the CHE model. By AIMD free energy sampling, we show that $CO_2 \rightarrow$ *COOH, the first step of CO_2RR, which is usually treated as a proton coupled electron transfer (PCET) step, is actually decoupled to an electron transfer (ET) step followed by a proton transfer (PT) step on FeN_4/C.[3] The CO_2 can only be activated to form a bent adsorbed *CO_2 under a more negative potential (Figure 2a), and the TS location also significantly shifts as the potential varies, similar to the case of *$N_2 \rightarrow$ *NNH in the NRR (vide infra). Note that this TS geometry is not obtainable with neutral-charge DFT calculations or without sufficient explicit solvation. Once the CO_2 is activated and adsorbed to the active site, the subsequent PT process is almost barrierless. In other words, the rate of $CO_2 \rightarrow$ *COOH is solely determined by the CO_2 activation ET step, and the failure of the CHE model to predict the overpotential of the CO_2RR is due to basing overpotential on the thermodynamics of the combined two steps. The CO_2 activation is an almost vertical reduction process, which has a potential dependence of barriers smaller than that of the rate-determining step (RDS) of the HER (Figure 2b), which leads to a crossover of selectivity at ca. −0.9 V, in line with the experimental observations.

Obtaining the correct potential dependence of reaction free energies underlies the success of rational design efforts. Based on the insights obtained from the CO_2RR on FeN_4/C, we further investigated the case of NiN_4/C with fine-tuned first-sphere coordination environments.[17] By altering the ratio of N and C in the first coordination sphere of the Ni center, the free energetics of the ET and PT steps can be tuned to achieve optimal overall kinetics of the CO_2RR. By microkinetic modeling based on the obtained potential dependent free energy profiles, NiN_1C_3/C is found to be the optimal pH-universal CO_2RR catalyst among the studies Ni SAEs.

An important implication from the above examples is that the reaction profile is not stationary at varying potentials; the location of the TS along the reaction coordinate changes at different potentials as a result of a reshaped free energy surface. In other words, the correct potential dependence of such an electrochemical reaction step could not be obtained by vertically charging/discharging each image along a neutral-charge minimum energy path. The shifting is most pronounced for reaction steps where the polarity of the adsorbate changes dramatically in the course of the reaction, such as the activation of N_2 (Figure 1) and CO_2 (Figure 2a). The reaction steps involving little change in polarity are less affected, such as *H desorption (Figure 2b). Since most electrocatalytic reactions involve both types of elementary steps (usually alternating), the rate-determining step could vary with potential, and the potential dependence of the TS location and barrier height could be highly inconsistent among elementary steps. An example is the inversion of water and dioxygen binding energy on the FeN_4 site as potential becomes more positive, which makes the step of dioxygen replacing adsorbed water the rate-limiting step, rather than the common belief of the hydrogenation step being rate-limiting.[18]

Note that all simulations discussed in this section as well as any similar works in the field employ a charge extrapolation scheme assuming a constant interfacial capacitance. In reality, the interfacial capacitance could vary along with the reorganization of the solvation layer and the chemical identity of the reaction intermediates, which are also potential dependent. There are some approaches that can obtain constant-potential energetics based on constant-charge energetics at very low costs, by adding an adaptive electric field correction[19] or by Legendre transformation.[20] However, these two approaches are based on a single transition path (usually from nudged elastic band calculation) with minimal solvation, which neglects completely the configurational changes and dynamics of the electrolyte along the reaction coordinate. Recent theoretical work has demonstrated that constant-charge and constant-potential ensembles are conjugated, and one can mathematically derive equilibrium constant-potential properties from a constant-charge trajectory.[21] This approach better accounts for the configurational entropy but still can fail in systems with phase transition-like potential dependent config-

https://doi.org/10.1021/acs.accounts.3c00589
Acc. Chem. Res. 2024, 57, 198−207

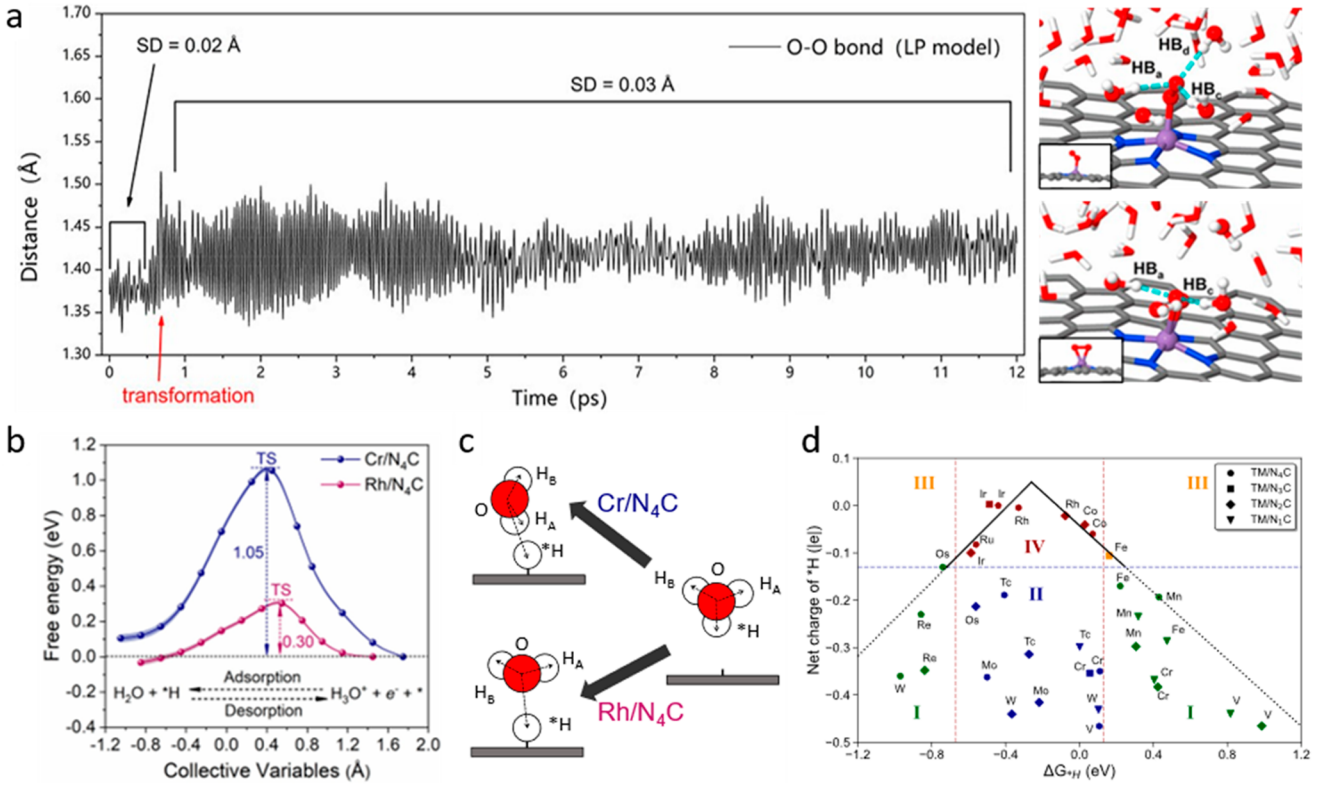

Figure 3. (a) Evolution of the O−O bond length in an $*O_2$ intermediate on MnN_4/C during AIMD simulation, with key snapshots shown on the right. Reproduced with permission from ref 24. Copyright 2020 American Chemical Society. (b) Free energy profiles and (c) initial and final state geometries of *H desorption on CrN_4/C and RhN_4/C. Reproduced with permission from ref 1. Copyright 2023 American Chemical Society. (d) Revised activity volcano plot considering kinetic effects. Reproduced with permission from ref 1. Copyright 2023 American Chemical Society.

urational changes.[1] A more rigorous treatment is to include an additional outer iteration, i.e., an imaginary potentiostat, to address the varying capacitance and extra charge in the system to achieve constant potential calculations of electronic free energies.[22] However, such methods are usually much more expensive than models based on the constant capacitance assumption and constant charge calculations, and there can still be unphysical behaviors in the potentiostat treatment. To date, it is still challenging to achieve accurate potential dependence (electronic free energy), configurational changes (entropic contribution to free energy, solvation, and dynamics), and low computational cost at the same time.

3. SOLVATION-MEDIATED ALTERNATIVE REACTION MECHANISMS

The polarity-dependent shift of the reaction profile arises from the interaction between the polar reaction intermediate and its neighboring water molecules via the highly directional H-bond interactions and adaptive H-bond networks. Although in most cases, the interaction only preferentially (de)stabilizes some reaction intermediates without altering the reaction mechanism, there exist cases where a qualitative change is induced.[23] One of the extreme cases is the chemisorption of dioxygen, the first step of the oxygen reduction reaction (ORR), on MnN_4/C.[24] As is shown in Figure 3a, the $*O_2$ transforms from a usually assumed terminal configuration into a side-on configuration spontaneously in an explicit water environment, accompanied by significant charge transfer from the catalyst to the adsorbate, during AIMD simulations. The side-on configuration also features a weaker O−O bond than in the terminal configuration. After protonation, the O−O bond in side-on $*O_2$ breaks to form *O and *OH on the Mn center (Figure 3a), rather than the usually assumed *OOH intermediate, similar to an earlier report by Li et al.[25] The alternative ORR reaction pathway has much lower energy barriers than the traditional *OOH pathway and is more consistent with the experimental overpotentials. This example highlights the stabilization of unconventional configurations of reaction intermediates, both energetically and geometrically, even on a single atom active site. Highly polar adsorbates with multiple possible binding configurations are expected to be subject to such configuration-altering changes, and it is worth revisiting common electrochemical reactions involving such intermediates.

The configuration of the solvent−intermediate complex around a reaction intermediate also plays a crucial role in determining the free energies. For example, *H atoms formed from hydronium on CrN_4/C and on RhN_4/C have almost identical configurations but very different free energies, with the barriers of adsorption being 1.05 eV on CrN_4/C but only 0.30 eV on RhN_4/C (Figure 3b).[1] This distinction originates in the configurational difference between their transition paths (Figure 3c): in the final state (*H + water), the water molecule over the *H on Rh/N_4C maintains an O-down configuration, which requires minimal movement as compared to the initial state; however, the water molecules over the *H on Cr/N_4C would need to flip to the H-down configuration, introducing an additional reorganization step and hence raising the free energy barrier. The orientation of the water molecule depends on the charge of the *H intermediate: earlier transition metals (Cr, Fe, Mn) tend to favor a more hydridic *H, which well serves as a

https://doi.org/10.1021/acs.accounts.3c00589
Acc. Chem. Res. 2024, 57, 198−207

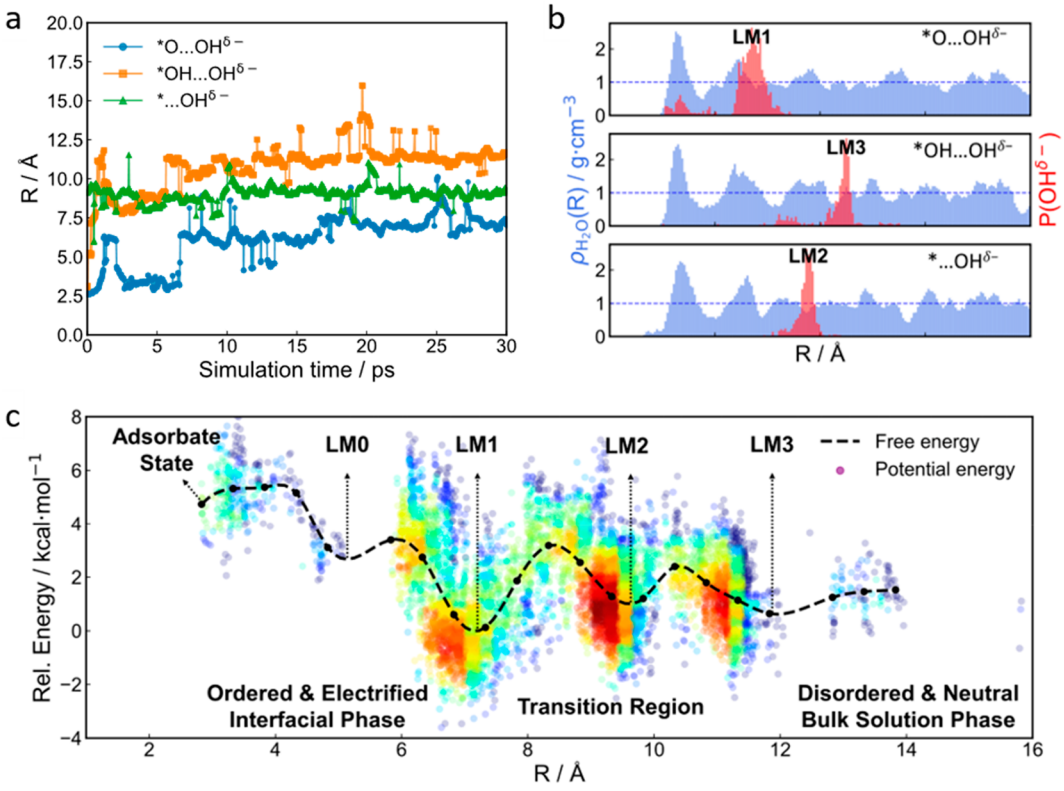

Figure 4. (a) Evolution of the pseudo-adsorbed hydroxide−surface distance and (b) spatial distribution of pseudo-adsorbed water and hydroxide during AIMD simulation for different ORR intermediates. (c) Free energy profile of hydroxide movement across the interface with key regions labeled. Reproduced with permission from ref 2. Copyright 2022 the Authors. Published by Springer Nature under a Creative Commons CC BY License.

strong H-bond acceptor and causes the water nearby to adopt a H-down orientation toward it; the late transition metals (Ru, Ir, Rh), however, could maintain a near-neutral *H and serve as a weak H-bond donor to stabilize the water overhead in its initial O-down orientation. In other words, the charges of *H atoms on metal centers are near the critical value between the making of a H-donor or -acceptor; hence even a subtle variation can induce a phase transition-like reorientation of the water molecule near the reaction intermediate and the reorganization of the H-bond networks beyond. The catalysts with a H-down water in their final states hence suffer from significant kinetic hindrance and exhibit bad HER/hydrogen oxidation reaction (HOR) performance despite favorable thermodynamics (ΔG_H). To better assess the activity of a single atom catalyst, both thermodynamic and kinetic metrics should be considered, and the resulting activity trend is far more complicated than a 1-dimensional activity volcano (Figure 3d). Note that our result is not a simple "shifting" of the HER activity volcano but inclusion of another dimension (Volmer kinetics) in the design space. Our revised model contains two descriptors, H binding energy for thermodynamics and net charge on *H for kinetics. The conventional HER activity volcano is valid only in the subspace of little kinetic hindrance. The original activity volcano model is after all a projection or cross-section of a higher dimension hypersurface to one single descriptor by considering only thermodynamics. By considering kinetics as well, which is decoupled from thermodynamics in some systems, we can recover the lost and projected-out degrees of freedom and unlock a large design space.

The studied kinetics−thermodynamics decorrelation is only accessible using a fully explicit solvation treatment, and it could in part explain the failure of the Brønsted−Evans−Polanyi (BEP) relation and the Sabatier principle in predicting activity trend of SACs: the more isolated active sites could host a more dramatic variation of local solvation configurations, which would translate to more significant kinetic effects which is often overlooked in simplified models.

4. INTERFACIAL DYNAMICS BEYOND THE CONTACT LAYER

The complex interfacial dynamics of solvent and reaction intermediates can take place far beyond the direct catalyst surface. During the AIMD simulation of ORR intermediates on FeN_4/C with full explicit solvation treatment, a dissociative mechanism is observed. Moreover, the hydroxide anion, as the result of *OOH dissociation, does not diffuse away into the bulk solution but stays within a few water layers over the catalyst surface, which we dubbed as a "pseudo-adsorption" state (Figure 4a).[2] More interestingly, the position of the pseudo-adsorbed hydroxide anion fluctuates during the course of the reaction, varying with different present reaction intermediates in a coupled manner (Figure 4b). Such variation along the reaction profile lies in the polarization of the catalyst/water interface, as is illustrated in Figure 4c. In the immediate vicinity of the reaction intermediate, the solvation shell is highly electrified and polarized to form a compact ordered phase which pushes the dissociated species outward (an entropic effect). Whereas in the bulk solution, the organization of water is neutral and disordered, offering little stabilization for the dissociated species. Between the two extremes a transition region emerges, where the solvation shell is ordered but not so compact, so that it affords an overall optimal stabilization effect and confine the

https://doi.org/10.1021/acs.accounts.3c00589
Acc. Chem. Res. 2024, 57, 198−207

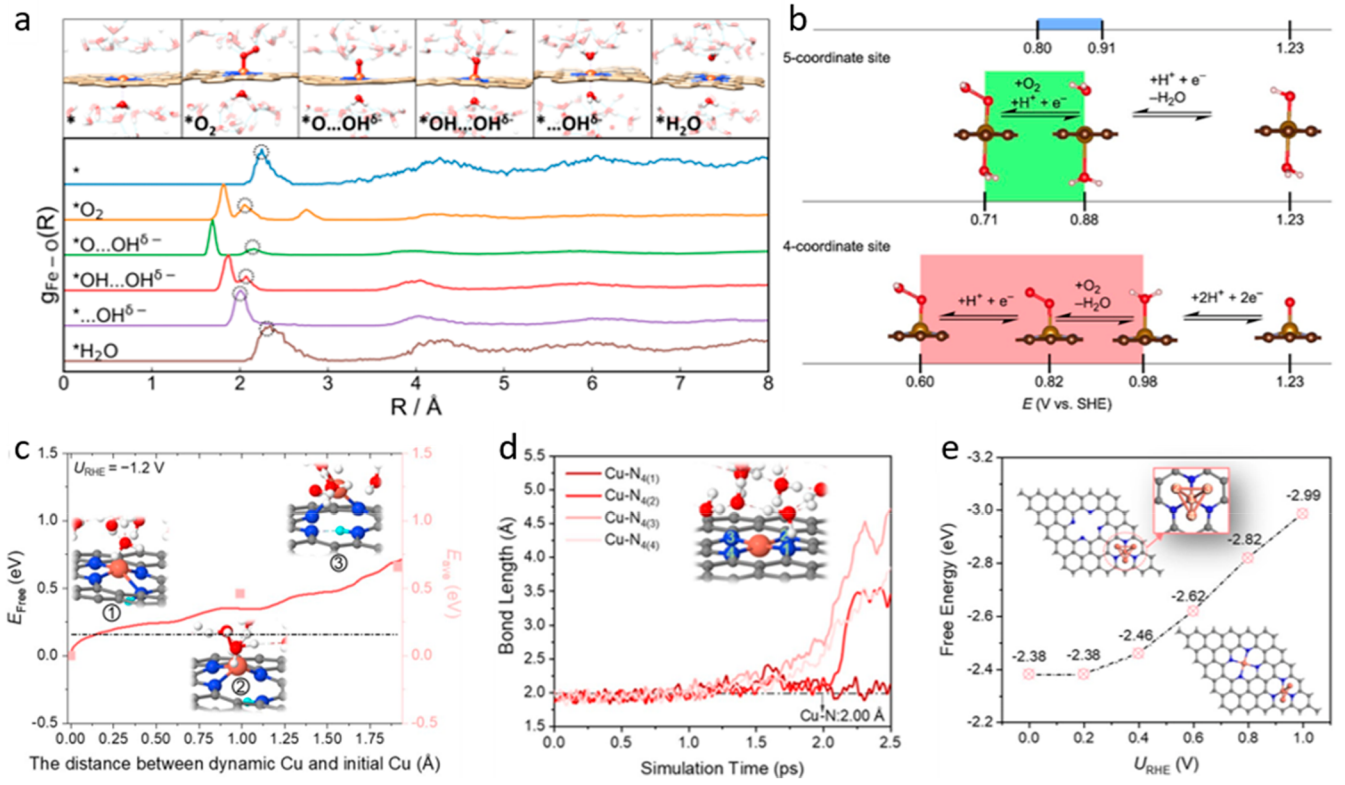

Figure 5. (a) Spatial distribution of the back side axial water during AIMD simulations for different ORR intermediates. Reproduced with permission from ref 2. Copyright 2022 the Authors. Published by Springer Nature under a Creative Commons CC BY License. (b) Predicted ORR overpotential window based on a single atom site with or without back side water ligand. Reproduced with permission from ref 26. Copyright 2022 American Chemical Society. (c) Free energy profile of Cu single atom dissolution upon protonation of the coordinating N. Reproduced with permission from ref 27. Copyright 2022 American Chemical Society. (d) Evolution of Cu−N bond lengths during AIMD simulation. Reproduced with permission from ref 27. Copyright 2022 American Chemical Society. (e) Potential-dependent free energy of Cu_4 cluster formation from Cu single atom sites. Reproduced with permission from ref 27. Copyright 2022 American Chemical Society.

hydroxide anion within a few water layers from the catalyst surface. The exact location of such an optimal transition region depends on the polarity of the reaction intermediate and its H-bond accepting/donating ability, i.e., how strongly it polarizes the interface and how far it can extend its effect. The hydroxide can then adaptively diffuse to the optimal region by proton exchange after/during each reaction step.

The dynamics of the pseudo-adsorbed hydroxide has more profound implications—how coupled is it to the reaction steps? This would depend on the specific time scale of the hydroxide diffusion (via proton exchange), reorganization of the first-shell solvents around the reaction intermediate, and the propagation of the polarization effect across the water layers, with respect to the time scale of the reaction steps. If the pseudo-adsorbed species diffuses much faster than the reaction steps, then we could assume that it could reach the equilibrium position (the global minimum on the free energy surface) after/during each reaction step. If such a case holds true, then the pseudo-adsorbed hydroxide and the water layers between it and the catalyst surface should all be included as part of the reaction system, due to the strongly coupled dynamics between the surface chemistry and the hydroxide diffusion. If it is much slower, then the hydroxide anion may not have enough time to diffuse away or even to break off from the *OOH intermediate, which brings the system back to the usually assumed surface-centered associative mechanism. If the events have similar time scales, then the pseudo-adsorbed hydroxide may be able to reach the equilibrium for some reaction intermediates but not for others: some intermediates that do not interact strongly enough with their solvation layers may fail to establish a large free energy gradient and to drive the diffusion of the pseudo-adsorbed species. We would not be able to quantify such time scales at this point, but the strongly coupled dynamics on a faraway solvated species with the catalyst surface is definitely intriguing and could be present in many common systems where the dissociated mechanism is likely.

5. DYNAMIC ACTIVATION AND DEACTIVATION MECHANISMS

In some cases, the interfacial dynamics can also interact strongly with the active center and alter its chemical nature. Taking the system of ORR on FeN_4/C as an example, if we consider the back side of the catalyst (the opposite side of the reaction intermediates) accessible to solvents, a water molecule can favorably coordinate to the metal center in the back side position and stay during the full course of the reaction.[2] Such coordination is relatively weak compared to a typical metal−oxygen bond, and it is more influenced by the identity of the reaction intermediate on the other side and the rearrangement of the solvation shell. As can be seen in Figure 5a, the radial distribution interaction (RDF) peak corresponding to the axial water ligand varies significantly in both bond length (location of the peak) and bond strength (width of the distribution), adapting to the chemical nature of the reaction intermediate

https://doi.org/10.1021/acs.accounts.3c00589
Acc. Chem. Res. 2024, 57, 198−207

present. The presence of the axial back side water ligand with adaptive coordination strength changes the ligand field of the active center from a square planar or pyramidal to a square dihedral one. As a result, the reaction energetics is improved by stabilization of key high-spin reaction intermediates, and the active center is prevented from M−N bond breakage and dissolution of metal content.[26] Considering the possible presence of axial ligands is hence crucial in understanding both the activity and stability of single atom catalysts.

By engineering the morphology of the catalyst, we could control the water accessibility to the back side. By creating defects of high concentration near the metal center, it is also possible to construct MN_5 sites, with one N coordinating from the graphitic layer below. Anionic or molecular additives could also be introduced to the catalyst to serve as back side ligands and to modify the reactivity of the metal center.

For CO_2RR on Cu SACs, the destabilized coordination environment of the active center is surprisingly the very origin of the reactivity.[27] Despite metallic Cu being an efficient CO_2RR catalyst, the CuN_4 motif itself is known to be inactive toward CO_2RR. However, under a reducing potential, the N ligand coordinating to the Cu center can be protonated to disrupt the CuN_4 moiety and cause the dissolution of the Cu center. Those dissolved Cu species can be preferentially reduced back at some other empty sites to nucleate into small Cu clusters (or nanostructures ultimately[28]) which exhibit CO_2RR activity. This is hypothesized to be the general mechanism of Cu-based SACs for electrocatalytic CO_2RR and highly resembles the case of dynamic single atom sites in thermal catalysis.[29] Even if the metal centers are not dissolved, there can still be a change in the coordination environment to achieve activation. It has been reported that, under the ORR conditions, the NiN_4 motif can transform into a near-free and partially reduced NiN_2 species, with two Ni−N bonds broken and the Ni center dangling slightly out-of-plane. Choi et al. have also recently reported a Pt SAE system where a minority species with a broken Pt-support bond (due to protonation of the coordinating C) exhibit broken symmetry and high electrocatalytic activity.[30]

It is likely that many other similar single atom electrocatalyst systems are subject to such dynamic activation mechanisms to different extents (dangling, dissolution, clustering). In general, a doped carbon support tends to weaken the anchoring of metal atoms when the coordination atoms are protonated, which promotes the metal center to a thermodynamically unstable undercoordinated state of higher reactivity. The weakened metal−support interaction can lead to demetalation, but the consequences can vary among systems−some metals would exhibit no activity once dissolved, but some may get redeposited and aggregate into clusters and particles which are responsible for the electrocatalysis. This calls for critically revisiting the structural dynamics of the single atom site and its coordination environments under an *operando* setting.

6. CHALLENGES, LIMITATIONS, AND HOW TO ADDRESS THEM

What we have examined in the discussed works is merely a small fraction of the vast complexity of the electrochemical interfaces. To achieve an accurate description of the electrocatalytic systems and to gain reliable fundamental insights, there are still many grand challenges. In this final section, we will discuss what obstacles lie ahead, the limit of current methods, and the future advances that could enable us to get over them.

An appropriate representation of the electrocatalyst is a prerequisite to any successful modeling efforts. A static model in the gas phase or with implicit solvation has been shown to be insufficient in accurately representing the SACs as discussed in the previous sections, and the realistic scenario can deviate qualitatively from the conventional understandings. Besides the interfacial dynamics, there are more factors that require more elaborate and sophisticated treatments: a prepared SAC contains not perfectly dispersed uniform MN_4 sites but a cocktail of many sites with various coordination environments, local active site density, and varied electrolyte accessibility.

Although a pre-reaction acid wash can remove the metal (nano)particles that formed during the synthesis, a reducing potential can usually induce reduction of the cationic active centers to metallic species of a broad distribution of size and morphology.[31]

Even if we assume the SA sites to be ideal (having perfect atomic dispersion and uniform coordination environments and being free from dissolution or agglomeration), metastable species can still form from the binding of adsorbates. Recently, it has been reported that Pt single atoms supported on indium tin oxide (ITO) would be covered by *O and *OH adsorbates to form a cationic $PtO(OH)_4$ species under oxygen evolution reaction (OER) conditions.[32] The heavy coverage of the O-containing adsorbates results from the relatively loose binding between Pt and ITO, which deviates significantly from that of bulk Pt and leads to an oxidation state of Pt as high as +2.66. This change in the chemical state of Pt is associated with a decrease of 0.3 V for the overpotential of the OER as compared to the model using a bare Pt SA.

Another usually overlooked aspect is the description of the electronic structure of the SA sites. MN_4 species, analogues to molecular pyrrolic or pyridinic transition metal complexes, are notorious for the complexity of their electronic structures. The interaction of the d states of the transition metal center and conducting bands of various substrates (usually graphitic or metallic) can give rise to strong electron correlations and difficulty in determining the correct multiplicity of the metal center.[33,34] Moreover, the MN_4 systems vary in their redox characteristics: some are metal-centered, some ligand-centered, and some redox-noninnocent.[35,36] Currently available computational methods often fail to provide a reliable picture of metal−support charge transfer for such reasons.

The varying oxidation states of the SA sites under the reaction conditions and the strong correlation also cast doubt on the use of the Hubbard model with a single U value, let alone pure functionals. More advanced multireference methods are required to describe these systems, which await the development of more computationally efficient algorithms and embedding methods for periodic systems.

The complexity at the electrochemical interface encompasses multiple factors of diverse origins and various effects: H-bond and other noncovalent interactions, compactness/iciness of the double layer, concentration of near-surface ions, the hardness of the hydration shell, electric fields, interfacial charge transfer, and so on.[37] "Solvation" is a phenomenological collective concept, after all. The factors could exert different effects on the reaction system, some competing and some synergistic. As many of the factors are intrinsically coupled to some others, it is challenging to separately investigate the effect of a single factor as a controlled variable without altering the others. A promising direction is to alter each experimentally controllable factor and probe the response of the electrochemical interface in order to

https://doi.org/10.1021/acs.accounts.3c00589
Acc. Chem. Res. 2024, 57, 198−207

categorize the factors into several somewhat independent groups by dimension reduction techniques or physical models. Simplified models of improved accuracy could be built based on the factor groups to understand the relative magnitude of each factor and to determine which one or ones are major factors under various reaction conditions.

Different factors could vary greatly in their characteristic time scales, spanning from tens of femtoseconds to seconds or even hours. The current capability of DFT can only achieve simulation of tens of picoseconds for a few hundreds of atoms, which is a rather small scale and insufficient to capture many events of interest. Long time scale events include the diffusion and hydration dynamics of ions (especially the heavier ones), reactive events, and other rare events such as major surface reconstruction and trapping in metastable states. The limited size of the models and the predefined periodicity also prohibit the study of long-range ordering, phase transition, step formation, and surface roughening. Moreover, rigorously quantifying the effect of a factor requires samples of equilibrium, which is unaffordable to reach for many events of longer time scale. A compromise is to sample near an assumed trapped state, which could serve as a "quasi-equilibrium" and yield semi-quantitative results to understand certain trends. In any case, the negligence of kinetic and interfacial factors could yield incorrect energetics and be misleading in reactivity trends.

To probe the structure of the single-site active centers, advanced electron microscopy methods such as cryogenic techniques, electron ptychography, and multidimensional real-space charge-density imaging have achieved subangstrom spatial resolution.[38−41] The *operando* electron microscopy techniques (electrochemical, environmental, etc.) have also enabled direct observation of the structural evolution during operation, but compromising some of the spatial-resolution. To address mechanistic questions, X-ray adsorption spectroscopy, with the ability to resolve the electronic structural features of active sites and reaction intermediates, has become an indispensable tool. Surface sensitive methods, such as surface enhanced Raman spectroscopy (SERS) and diffuse reflectance infrared spectroscopy (DRIFTS), also have the ability to capture the change in surface state and signals of reaction intermediates. However, the processes within reach of the theory are often beyond the temporal resolution of current instrumentation, especially the formation and evolution of metastable surface species with short lifetimes. Long-range interfacial phenomena, which can span the range of the whole electric double layer and involve transient solvated species, are also challenging to detect with spectroscopic methods. Even if detectable, the signals of the metastable species can be so weak that they are convoluted and overwhelmed by bulk signals and noise, especially on catalysts with dynamic single-atom active sites. Hence, many of the gained atomistic insights discussed in this work are beyond the resolution of *in situ* characterization techniques, which makes the role of theory unique and singular in elucidating the atomistic mechanisms.

Many of the mentioned challenges above could benefit from the development of machine learning models. Machine learning interatomic potentials could greatly accelerate the exploration of the potential energy surface, which enables extensive sampling of complex reconstructed surfaces with mixed adsorbate coverages and long time scale molecular dynamics simulations of very large systems.[42−44] For systems involving more complicated interactions or with strong correlations, machine learning can also help determine the optimal functional and hyperparameters to improve overall accuracy and speed.[45,46] In addition, machine learning models can extract descriptors out of the many properties of a catalyst system to accelerate virtual screening and rational design.[33,47] The ensemble representation combined with machine learning models have also been demonstrated to be powerful for interpreting *in situ* spectroscopic signals of complex systems.[48−50] However, there are still several challenges lying ahead for the application of ML in designing SAEs: (1) The representation of SAEs are usually simplistic without consideration of dynamics at the active center and at the interface. (2) The upper limit of the accuracy of the trained DFT models is that of the training set (usually DFT), so ML can never capture anything out of scope for the DFT, such as complexity of the electronic structure, some are not well described by regular DFT and require more advanced treatments.[51] (3) ML interatomic potentials cannot address constant-potential simulations where the number of electrons fluctuates and the system effectively travels multiple potential energy surfaces upon charge transfer. (3) The unconventional pathways (the ones highlighted in this Account) are not in the training set nor in the representations; hence the optimization using ML would be confined in a predefined search space limited by the prior work.

In this Account, we provide an overview of recent findings on the critical role of solvation and electrode potential in modeling the dynamics and free energetics of SAEs, with discussions on their implications, challenges, and possible solutions. We illustrate that the SAEs, despite a relatively simple structure, have dynamic behaviors, ensemble phenomena, and interfacial chemistry as rich as those of restructuring clusters and surfaces. By leveraging state-of-the-art computational tools, we show that it is now possible to include realistic factors into the model to better understand activity and selectivity trends, elucidate reaction mechanisms, and revise SAE design principles.

We highlight the importance and benefits of removing the convenient assumptions and recovering the dynamics and realistic factors that are removed in the popular simplistic activity models whenever possible. Only by doing so can we identify the applicability of the simplistic models, so that we can use them more confidently in the systems where they hold, and revise or reinvent them for the systems where they do not. The methods discussed here may seem overkill at the moment, but we believe they will become routine calculations in a decade or two. Just as periodic DFT calculations became routine and gave rise to the CHE and activity volcanoes, the methods considering the full complexity of electrochemical interfaces would form the basis for developing next-generation activity models for the design of SAEs with activity, selectivity, and stability beyond the upper limit of existing design principles.

We hope this Account can inspire the modeling community to face, understand, address, and make use of the complexity of the electrochemical interface to unlock rich interfacial chemistry and open up hidden dimensions for catalyst design. It is worth the effort to go down this rabbit hole.

AUTHOR INFORMATION

Corresponding Author

Yang-Gang Wang − *Department of Chemistry and Guangdong Provincial Key Laboratory of Catalytic Chemistry, Southern University of Science and Technology, Shenzhen 518055 Guangdong, China;* orcid.org/0000-0002-0582-0855; Email: wangyg@sustech.edu.cn

https://doi.org/10.1021/acs.accounts.3c00589
Acc. Chem. Res. 2024, 57, 198−207

Authors

Zisheng Zhang − *Department of Chemistry, Southern University of Science and Technology, Shenzhen 518055 Guangdong, China; Department of Chemistry and Biochemistry, University of California, Los Angeles, Los Angeles, California 90095, United States;* orcid.org/0000-0002-4370-4038

Jun Li − *Department of Chemistry and Guangdong Provincial Key Laboratory of Catalytic Chemistry, Southern University of Science and Technology, Shenzhen 518055 Guangdong, China; Department of Chemistry and Key Laboratory of Organic Optoelectronics & Molecular Engineering of Ministry of Education, Tsinghua University, Beijing 100084, China;* orcid.org/0000-0002-8456-3980

Complete contact information is available at: https://pubs.acs.org/10.1021/acs.accounts.3c00589

Notes

The authors declare no competing financial interest.

Biographies

Zisheng Zhang was born in Wuhan in 1997. He received a B.Sc. in Chemistry from Southern University of Science and Technology of China in 2019, advised by Prof. Jun Li and Prof. Yang-Gang Wang. At University of California, Los Angeles (UCLA), he was a UCLA-CSST fellow in 2019, obtained a M.Sc. in Chemistry in 2021, and expects to receive his Ph.D. in Theoretical and Computational Chemistry in 2024, advised by Prof. Anastassia N. Alexandrova. His research interests include realistic modeling of dynamic catalytic interfaces and inverse design of functional molecules.

Jun Li received his Ph.D. degree in Physical Chemistry from Fujian Institute of Research on the Structure of Matter, Chinese Academy of Sciences, in 1992. He did postdoctoral research at the University of Siegen (Germany) and The Ohio State University (USA) from 1994 to 1997. He worked as a Research Scientist at The Ohio State University as well as Senior Research Scientist and Staff Scientist at the Pacific Northwest National Laboratory from 1997 to 2009. He is now a full professor in the Department of Chemistry, Tsinghua University. He is an elected AAAS Fellow and Chinese Chemical Society Fellow. His research involves theoretical chemistry, heavy-element quantum chemistry, and computational catalysis science.

Yang-Gang Wang received his Ph.D. degree from Tsinghua University in 2014, supervised by Prof. Jun Li. After that, he worked as a postdoctoral research fellow at Pacific Northwest National Laboratory (USA) under the supervision of Dr. Roger Rousseau and Dr. Vassiliki-Alexander Glezakou until 2016. Then he became a Humboldt research fellow at Fritz Haber Institute and worked with Dr. Sergey Levchenko and Prof. Matthias Scheffler until 2018. He is currently an associate professor at Southern University of Science and Technology. His research interests focus on the development of theory and simulation for dynamic catalysis under realistic conditions.

■ ACKNOWLEDGMENTS

This work was financially supported by NSFC (Nos. 22022504 and 22373045) of China, Guangdong "Pearl River" Talent Plan (No. 2019QN01L353), Science, Technology and Innovation Commission of Shenzhen Municipality (Nos. KCXST20221021111207017 and JCYJ20210324103608023), and Guangdong Provincial Key Laboratory of Catalysis (No. 2020B121201002).

■ REFERENCES

(1) Cao, H.; Wang, Q.; Zhang, Z.; Yan, H. M.; Zhao, H.; Yang, H. B.; Liu, B.; Li, J.; Wang, Y. G. Engineering Single-Atom Electrocatalysts for Enhancing Kinetics of Acidic Volmer Reaction. *J. Am. Chem. Soc.* **2023**, *145*, 13038−13047.

(2) Chen, J.-W.; Zhang, Z.; Yan, H.-M.; Xia, G.-J.; Cao, H.; Wang, Y.-G. Pseudo-Adsorption and Long-Range Redox Coupling during Oxygen Reduction Reaction on Single Atom Electrocatalyst. *Nat. Commun.* **2022**, *13*, 1734.

(3) Cao, H.; Zhang, Z.; Chen, J.-W.; Wang, Y.-G. Potential-Dependent Free Energy Relationship in Interpreting the Electrochemical Performance of CO_2 Reduction on Single Atom Catalysts. *ACS Catal.* **2022**, *12*, 6606−6617.

(4) Qian, S.-J.; Cao, H.; Chen, J.-W.; Chen, J.-C.; Wang, Y.-G.; Li, J. Critical Role of Explicit Inclusion of Solvent and Electrode Potential in the Electrochemical Description of Nitrogen Reduction. *ACS Catal.* **2022**, *12*, 11530−11540.

(5) Asakura, K.; Nagahiro, H.; Ichikuni, N.; Iwasawa, Y. Structure and Catalytic Combustion Activity of Atomically Dispersed Pt Species at MgO Surface. *Appl. Catal. A Gen.* **1999**, *188*, 313−324.

(6) Qiao, B.; Wang, A.; Yang, X.; Allard, L. F.; Jiang, Z.; Cui, Y.; Liu, J.; Li, J.; Zhang, T. Single-Atom Catalysis of CO Oxidation Using Pt1/FeOx. *Nat. Chem.* **2011**, *3*, 634−641.

(7) Li, X.; Yang, X.; Huang, Y.; Zhang, T.; Liu, B. Supported Noble-Metal Single Atoms for Heterogeneous Catalysis. *Adv. Mater.* **2019**, *31*, 1902031.

(8) Flytzani-Stephanopoulos, M.; Gates, B. C. Atomically Dispersed Supported Metal Catalysts. *Annu. Rev. Chem. Biomol. Eng.* **2012**, *3*, 545−574.

(9) Deng, D.; Chen, X.; Yu, L.; Wu, X.; Liu, Q.; Liu, Y.; Yang, H.; Tian, H.; Hu, Y.; Du, P.; Si, R.; Wang, J.; Cui, X.; Li, H.; Xiao, J.; Xu, T.; Deng, J.; Yang, F.; Duchesne, P. N.; Zhang, P.; Zhou, J.; Sun, L.; Li, J.; Pan, X.; Bao, X. A Single Iron Site Confined in a Graphene Matrix for the Catalytic Oxidation of Benzene at Room Temperature. *Sci. Adv.* **2015**, *1*, No. e1500462.

(10) Liu, J. Catalysis by Supported Single Metal Atoms. *ACS Catal.* **2017**, *7*, 34−59.

(11) Wang, A.; Li, J.; Zhang, T. Heterogeneous Single-Atom Catalysis. *Nat. Rev. Chem.* **2018**, *2*, 65.

(12) Zhao, X.; Levell, Z. H.; Yu, S.; Liu, Y. Atomistic Understanding of Two-Dimensional Electrocatalysts from First Principles. *Chem. Rev.* **2022**, *122*, 10675−10709.

(13) Exner, K. S.; Over, H. Kinetics of Electrocatalytic Reactions from First-Principles: A Critical Comparison with the Ab Initio Thermodynamics Approach. *Acc. Chem. Res.* **2017**, *50*, 1240−1247.

(14) Abidi, N.; Lim, K. R. G.; Seh, Z. W.; Steinmann, S. N. Atomistic Modeling of Electrocatalysis: Are We There Yet? *Wiley Interdiscip. Rev. Comput. Mol. Sci.* **2021**, *11*, No. e1499.

(15) Rossmeisl, J.; Skúlason, E.; Björketun, M. E.; Tripkovic, V.; Nørskov, J. K. Modeling the Electrified Solid-Liquid Interface. *Chem. Phys. Lett.* **2008**, *466*, 68−71.

(16) Chan, K.; Nørskov, J. K. Potential Dependence of Electrochemical Barriers from Ab Initio Calculations. *J. Phys. Chem. Lett.* **2016**, *7*, 1686−1690.

(17) Zhao, H.; Cao, H.; Zhang, Z.; Wang, Y.-G. Modeling the Potential-Dependent Kinetics of CO2 Electroreduction on Single-Nickel Atom Catalysts with Explicit Solvation. *ACS Catal.* **2022**, *12*, 11380−11390.

(18) Yu, S.; Levell, Z.; Jiang, Z.; Zhao, X.; Liu, Y. What Is the Rate-Limiting Step of Oxygen Reduction Reaction on Fe-N-C Catalysts? *J. Am. Chem. Soc.* **2023**, *145*, 25352−25356.

(19) Luan, D.; Xiao, J. Adaptive Electric Fields Embedded Electrochemical Barrier Calculations. *J. Phys. Chem. Lett.* **2023**, *14*, 685−693.

(20) Beinlich, S. D.; Kastlunger, G.; Reuter, K.; Hörmann, N. G. Controlled Electrochemical Barrier Calculations without Potential Control. *J. Chem. Theory Comput.* **2023**, *19*, 8323.

(21) Tee, S. R.; Searles, D. J. Constant Potential and Constrained Charge Ensembles for Simulations of Conductive Electrodes. *J. Chem. Theory Comput.* **2023**, *19*, 2758−2768.
(22) Lv, X.-M.; Zhao, H.-Y.; Wang, Y.-G. Continuous Constant Potential Model for Describing the Potential-Dependent Energetics of CO2RR on Single Atom Catalysts. *J. Chem. Phys.* **2023**, *159*, 94109.
(23) Tosoni, S.; Di Liberto, G.; Matanovic, I.; Pacchioni, G. Modelling Single Atom Catalysts for Water Splitting and Fuel Cells: A Tutorial Review. *J. Power Sources* **2023**, *556*, 232492.
(24) Cao, H.; Xia, G. J.; Chen, J. W.; Yan, H. M.; Huang, Z.; Wang, Y. G. Mechanistic Insight into the Oxygen Reduction Reaction on the Mn-N4/C Single-Atom Catalyst: The Role of the Solvent Environment. *J. Phys. Chem. C* **2020**, *124*, 7287−7294.
(25) Zhong, L.; Li, S. Unconventional Oxygen Reduction Reaction Mechanism and Scaling Relation on Single-Atom Catalysts. *ACS Catal.* **2020**, *10*, 4313−4318.
(26) Hutchison, P.; Rice, P. S.; Warburton, R. E.; Raugei, S.; Hammes-Schiffer, S. Multilevel Computational Studies Reveal the Importance of Axial Ligand for Oxygen Reduction Reaction on Fe-N-C Materials. *J. Am. Chem. Soc.* **2022**, *144*, 16524−16534.
(27) Bai, X.; Zhao, X.; Zhang, Y.; Ling, C.; Zhou, Y.; Wang, J.; Liu, Y. Dynamic Stability of Copper Single-Atom Catalysts under Working Conditions. *J. Am. Chem. Soc.* **2022**, *144*, 17140−17148.
(28) Weng, Z.; Wu, Y.; Wang, M.; Jiang, J.; Yang, K.; Huo, S.; Wang, X. F.; Ma, Q.; Brudvig, G. W.; Batista, V. S.; Liang, Y.; Feng, Z.; Wang, H. Active Sites of Copper-Complex Catalytic Materials for Electrochemical Carbon Dioxide Reduction. *Nat. Commun.* **2018**, *9*, 415.
(29) Wang, Y.-G.; Mei, D.; Glezakou, V.-A.; Li, J.; Rousseau, R. Dynamic Formation of Single-Atom Catalytic Active Sites on Ceria-Supported Gold Nanoparticles. *Nat. Commun.* **2015**, *6*, 6511.
(30) Cho, J.; Lim, T.; Kim, H.; Meng, L.; Kim, J.; Lee, S.; Lee, J. H.; Jung, G. Y.; Lee, K.-S.; Viñes, F.; Illas, F.; Exner, K. S.; Joo, S. H.; Choi, C. H. Importance of Broken Geometric Symmetry of Single-Atom Pt Sites for Efficient Electrocatalysis. *Nat. Commun.* **2023**, *14*, 3233.
(31) Guo, Y.; Wang, M.; Zhu, Q.; Xiao, D.; Ma, D. Ensemble Effect for Single-Atom, Small Cluster and Nanoparticle Catalysts. *Nat. Catal.* **2022**, *5*, 766−776.
(32) Kumari, S.; Sautet, P. Elucidation of the Active Site for the Oxygen Evolution Reaction on a Single Pt Atom Supported on Indium Tin Oxide. *J. Phys. Chem. Lett.* **2023**, *14*, 2635−2643.
(33) Zhang, Z.; Wang, Y.-G. Molecular Design of Dispersed Nickel Phthalocyanine@Nanocarbon Hybrid Catalyst for Active and Stable Electroreduction of CO2. *J. Phys. Chem. C* **2021**, *125*, 13836−13849.
(34) Kaminsky, C. J.; Weng, S.; Wright, J.; Surendranath, Y. Adsorbed Cobalt Porphyrins Act like Metal Surfaces in Electrocatalysis. *Nat. Catal.* **2022**, *5*, 430−442.
(35) Wu, Y.; Jiang, J.; Weng, Z.; Wang, M.; Broere, D. L. J.; Zhong, Y.; Brudvig, G. W.; Feng, Z.; Wang, H. Electroreduction of CO2 Catalyzed by a Heterogenized Zn-Porphyrin Complex with a Redox-Innocent Metal Center. *ACS Cent. Sci.* **2017**, *3*, 847−852.
(36) Zhang, X.; Wang, Y.; Gu, M.; Wang, M.; Zhang, Z.; Pan, W.; Jiang, Z.; Zheng, H.; Lucero, M.; Wang, H.; Sterbinsky, G. E.; Ma, Q.; Wang, Y. G.; Feng, Z.; Li, J.; Dai, H.; Liang, Y. Molecular Engineering of Dispersed Nickel Phthalocyanines on Carbon Nanotubes for Selective CO2 Reduction. *Nat. Energy* **2020**, *5*, 684−692.
(37) Shah, A. H.; Zhang, Z.; Huang, Z.; Wang, S.; Zhong, G.; Wan, C.; Alexandrova, A. N.; Huang, Y.; Duan, X. The Role of Alkali Metal Cations and Platinum-Surface Hydroxyl in the Alkaline Hydrogen Evolution Reaction. *Nat. Catal.* **2022**, *5*, 923−933.
(38) Chen, Z.; Odstrcil, M.; Jiang, Y.; Han, Y.; Chiu, M.-H.; Li, L.-J.; Muller, D. A. Mixed-State Electron Ptychography Enables Sub-Angstrom Resolution Imaging with Picometer Precision at Low Dose. *Nat. Commun.* **2020**, *11*, 2994.
(39) Jiang, Y.; Chen, Z.; Han, Y.; Deb, P.; Gao, H.; Xie, S.; Purohit, P.; Tate, M. W.; Park, J.; Gruner, S. M.; et al. Electron Ptychography of 2D Materials to Deep Sub-Ångström Resolution. *Nature* **2018**, *559*, 343−349.
(40) Gao, W.; Addiego, C.; Wang, H.; Yan, X.; Hou, Y.; Ji, D.; Heikes, C.; Zhang, Y.; Li, L.; Huyan, H.; Blum, T.; Aoki, T.; Nie, Y.; Schlom, D. G.; Wu, R.; Pan, X. Real-Space Charge-Density Imaging with Sub-Ångström Resolution by Four-Dimensional Electron Microscopy. *Nature* **2019**, *575*, 480−484.
(41) Li, Y.; Huang, W.; Li, Y.; Chiu, W.; Cui, Y. Opportunities for Cryogenic Electron Microscopy in Materials Science and Nanoscience. *ACS Nano* **2020**, *14*, 9263−9276.
(42) Marcella, N.; Lim, J. S.; Płonka, A. M.; Yan, G.; Owen, C. J.; van der Hoeven, J. E. S.; Foucher, A. C.; Ngan, H. T.; Torrisi, S. B.; Marinkovic, N. S.; et al. Decoding Reactive Structures in Dilute Alloy Catalysts. *Nat. Commun.* **2022**, *13*, 832.
(43) Sumaria, V.; Sautet, P. CO Organization at Ambient Pressure on Stepped Pt Surfaces: First Principles Modeling Accelerated by Neural Networks. *Chem. Sci.* **2021**, *12*, 15543−15555.
(44) Lim, J. S.; Vandermause, J.; van Spronsen, M. A.; Musaelian, A.; Xie, Y.; Sun, L.; O'Connor, C. R.; Egle, T.; Molinari, N.; Florian, J.; Duanmu, K.; Madix, R. J.; Sautet, P.; Friend, C. M.; Kozinsky, B. Evolution of Metastable Structures at Bimetallic Surfaces from Microscopy and Machine-Learning Molecular Dynamics. *J. Am. Chem. Soc.* **2020**, *142*, 15907−15916.
(45) Ju, C.-W.; French, E. J.; Geva, N.; Kohn, A. W.; Lin, Z. Stacked Ensemble Machine Learning for Range-Separation Parameters. *J. Phys. Chem. Lett.* **2021**, *12*, 9516−9524.
(46) Duan, C.; Nandy, A.; Meyer, R.; Arunachalam, N.; Kulik, H. J. A Transferable Recommender Approach for Selecting the Best Density Functional Approximations in Chemical Discovery. *Nat. Comput. Sci.* **2023**, *3*, 38−47.
(47) Zhang, Z.; Hermans, I.; Alexandrova, A. N. Off-Stoichiometric Restructuring and Sliding Dynamics of Hexagonal Boron Nitride Edges in Conditions of Oxidative Dehydrogenation of Propane. *J. Am. Chem. Soc.* **2023**, *145*, 17265−17273.
(48) Timoshenko, J.; Halder, A.; Yang, B.; Seifert, S.; Pellin, M. J.; Vajda, S.; Frenkel, A. I. Subnanometer Substructures in Nanoassemblies Formed from Clusters under a Reactive Atmosphere Revealed Using Machine Learning. *J. Phys. Chem. C* **2018**, *122*, 21686−21693.
(49) Timoshenko, J.; Ahmadi, M.; Roldan Cuenya, B. Is There a Negative Thermal Expansion in Supported Metal Nanoparticles? An in Situ X-Ray Absorption Study Coupled with Neural Network Analysis. *J. Phys. Chem. C* **2019**, *123*, 20594−20604.
(50) Timoshenko, J.; Frenkel, A. I. "Inverting" X-Ray Absorption Spectra of Catalysts by Machine Learning in Search for Activity Descriptors. *ACS Catal.* **2019**, *9*, 10192−10211.
(51) Liu, J.-C.; Luo, F.; Li, J. Electrochemical Potential-Driven Shift of Frontier Orbitals in M-N-C Single-Atom Catalysts Leading to Inverted Adsorption Energies. *J. Am. Chem. Soc.* **2023**, *145*, 25264−25273.

https://doi.org/10.1021/acs.accounts.3c00589
Acc. Chem. Res. 2024, 57, 198−207